ADAPTIVE OPTICAL SYSTEMS. METHODS OF PHASE–FRONT RECONSTRUCTION AND DEVELOPMENT OF SYSTEM STRUCTURE AND NEW ELEMENT BASE (REVIEW OF PUBLISHED WORKS)

D.A. Bezuglov, E.N. Mishchenko, and S.E. Mishchenko

M.I. Nedelin Rostov Higher Military Command–Engineering School for the Rocket Forces
Received August 16, 1994

Theoretical and practical aspects of the development of adaptive optical systems, new element base, methods, and algorithms are considered in the paper based on recent publications of the authors.

1. INTRODUCTION

Today the utility and necessity of employing a wide range of optical systems, e.g., telescopes, optical detection and ranging systems, industrial high–power laser installations, etc., are beyond question. Workers concerned with the problems of improving the performance and enhancing the potential of such systems are faced with a spectrum of applied scientific problems. A central problem is the compensation for nonstationary phase perturbations caused by the atmosphere. Optical signal distortions caused by inhomogeneities in the refractive index of a propagation medium adversely affect the performance characteristics of optical systems and telescopes and make it impossible to attain rated precision. In case of direct photodetection the signal–to–noise ratio of information and measuring systems significantly decreases, and in some instances the adverse effect of the turbulence interferes with heterodyne reception.

Linnick and Babcock pioneered a new line of inquiry referred to as adaptive optics. The operation of adaptive optical systems (AOS's) in the widest sense consists in direct or indirect measurement of the spatial distribution of field amplitude and phase on the AOS aperture and construction of an algorithm optimum against a specified criterion, which in this case allows one to compensate to a significant extent for the adverse effect of the turbulence thereby providing preset performance of AOS. Of special note are the studies of Russian and foreign scientists who have theoretically and experimentally shown that in the majority of cases the only means of compensating for the adverse effect of the turbulence is the adaptive control of optical radiation phase. Neither postdetector processing with recording of optical signal energy nor various methods of photographic image processing are efficient.

This review gives our main results obtained in recent years. The avenue of investigation was determined by specific engineering problems. It should be immediately specified that we do not pretend to give a full and comprehensive treatment of the problem of AOS development.

Investigations are carried out by us along the following lines:
– construction of faster multidither and phase conjugation algorithms;
– development of methods of phase front reconstruction from measurements of the intensity of the Fourier transform of a light field;

– development of cumulant methods of assessing AOS potential;
– working out of new design approaches to the development of element base of adaptive optics;
– development of new AOS structure based on synthesized algorithms.

2. CONSTRUCTION OF FASTER MULTIDITHER AND PHASE CONJUGATION ALGORITHMS

For practical implementation of multidither method the aperture of an optical system is generally divided into N subapertures, each performing spatial modulation of the incident wave phase. Test actions, as a rule, are applied to all apertures simultaneously, with modulation frequency being different in each particular instant.[1–3] The majority of systems with multichannel phase modulation make use of one or other methods of selection of control signals that are proportional to the intensity gradient of a point photodetector. In the optimization theory, such algorithms are classified as first–order algorithms.

A further analysis of algorithms calls for a distinction in type of an adaptive mirror used in AOS. When a segmented phase–front corrector is used, faster algorithms can be provided by a second–order algorithm,[1] which essentially takes into account the second derivative of the intensity with respect to the control coordinates

$$\mathbf{B}_{i+1} = \mathbf{B}_i + C' \, \mathbf{\Gamma}_i , \qquad (1)$$

where $\mathbf{B}_i$ is the column vector of control signals at the ith step, C' is the matrix of the coefficients

$$C'_{nk} = \begin{cases} 1/(N+1) , \ n = k \\ 2/(N+1) , \ n \neq k \end{cases}$$, and $\mathbf{\Gamma}_i$ is the intensity gradient (vector whose components are the output signals of AOS band–pass filters).

When flexible mirrors, e.g., membrane–type ones, are used in AOS, one more problem arises[3] in addition to poor convergence of the multidither algorithms, viz., control voltage applied to an actuator of a flexible mirror causes its deformation at the clamping points of the rest of the actuators. This problem stems from the fact that a flexible membrane is a distributed system. To solve this problem, the geometry of an adaptive mirror should be taken into account along with implementation of a second–order algorithm.[1] In this case the notion of flexibility matrix is generally introduced for the adaptive mirror F with the segments f_{ij}. The physical meaning of

　　　　　　　　© 1995 　Institute 　of 　Atmospheric 　Optics

this matrix is that it describes the response of a flexible mirror when control voltage is applied to the ith actuator, with the f_{ij} matrix components being equal to the deformation of the mirror at the jth point. Obviously, if such a matrix could be experimentally or theoretically obtained for a specific adaptive mirror, then an inverse matrix F^{-1} could be calculated, and by multiplying the vector of control signals of the form (1) by F^{-1} a second–order algorithm could be obtained, which takes into account the geometry of the mirror and preserves all its advantages. This algorithm described in detail in Ref. 2 is likely to be most efficient when combinations of piezoelectric plates of different shapes are used as adaptive mirrors. However, neglect of the geometry of membrane–type and flexible piezoelectric mirrors in this case may make AOS completely inoperative.

Examination of the second–order multidither algorithms from the standpoint of their execution speed[1–2] has shown that their implementation allows significant increase of the speed of AOS operation (in some instances by a factor of several tens). It should be emphasized that the use of control in the transformed coordinates and the F^{-1} matrix may render the stability of the process of search for a global extreme.

In addition to the multidither methods, a technique of phase conjugation is also known, in which phase distribution on the aperture of an optical system is directly measured, the vector of control signals is computed, and finally, the phase front is corrected by means of an adaptive mirror against a specified criterion. In this case designers of optical systems have to cope with a number of problems. First, direct measurement of phase distribution is unfeasible. Second, phase data array measured at different points of the aperture has to be converted into the vector of control signals of an adaptive mirror. This is due to different dimensionality and basis of the calculated phase distribution and those of the adaptive mirror.

Moreover, as in the former case, type of adaptive mirror used in AOS should be taken into account when algorithms of phase conjugation are synthesized. Classification of algorithms for indirect measurement of phase–front parameters is shown in Fig. 1. Let us consider in detail the mathematical methods of phase–front reconstruction from measurements of local tilts. Methods of amplitude distribution conversion are also considered below.

In AOS with a segmented phase–front corrector and shift control[4] or shift and tilt control,[5] it is expedient to use the algorithm of piecewise linear approximation described in Ref. 6, while in AOS with a flexible membrane–type mirror, implementation of the algorithm for phase–front reconstruction based on normalized B–splines[7,8,9] yields the best results. When a modal corrector is used as a phase–front corrector, it is expedient to implement an algorithm from Ref. 10, which allows one to obtain directly the vector of coefficients at Zernike polynomials from an array of measured local tilts of the phase front. The algorithms described in Refs. 6–10 entail significantly reduced volume of calculation as compared with the ones known thus far and ensure phase–front reconstruction with preassigned accuracy. They can be easy implemented with the use of compute facilities.
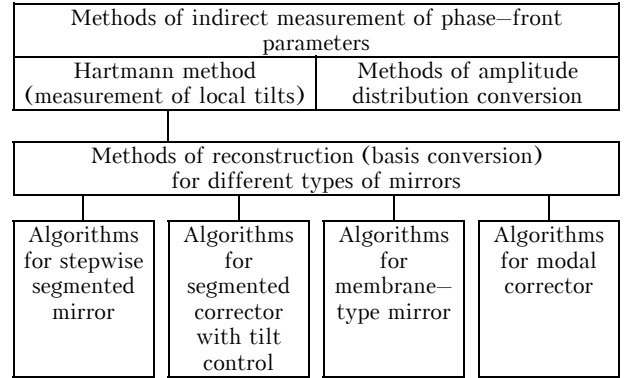
Methods of indirect measurement of phase–front parameters	
Hartmann method (measurement of local tilts)	Methods of amplitude distribution conversion

Methods of reconstruction (basis conversion) for different types of mirrors			
Algorithms for stepwise segmented mirror	Algorithms for segmented corrector with tilt control	Algorithms for membrane–type mirror	Algorithms for modal corrector

FIG. 1. Classification of algorithms for phase conjugation.

3. METHODS FOR PHASE–FRONT RECONSTRUCTION FROM MEASUREMENTS OF THE INTENSITY OF THE FOURIER TRANSFORM OF A LIGHT FIELD

When the algorithms for phase–front reconstruction were considered in the previous section, mention was made of the methods based on measuring amplitude distribution[8] in several cross sections. Two methods discussed below[11,12] are illustrative in this respect.

Let us introduce designations for complex amplitude distribution on the aperture of an input optical beam, i.e.,

$$F(x, y) = A(x, y) \exp\left(-i\varphi(x, y)\right), \qquad (2)$$

where $A(x, y)$ and $\varphi(x, y)$ are the amplitude and phase distribution on the aperture of an optical system, respectively. By intensity in this case is meant

$$I_1(x, y) = |F(x, y) F^*(x, y)|^2 = A^2(x, y). \qquad (3)$$

Let us derive the expression for the intensity after differentiation of the input beam

$$I_2(x, y) = \frac{\partial}{\partial x} F(x, y)|^2 = \left[\frac{\partial A^*(x,y)}{\partial x}\right]^2 + A^{*2}(x, y)\left[\frac{\partial \varphi(x,y)}{\partial x}\right]^2, \qquad (4)$$

where $A^*(x, y) = cA(x, y)$, c is a constant coefficient which specifies the losses of the amplitude after differentiation.

The expression for the desired phase–front tilts along the x coordinate can be derived from Eq. (4)

$$\frac{\partial \varphi(x, y)}{\partial x} = \frac{\left\{I_2(x, y) - \left[\frac{\partial A^*(x, y)}{\partial x}\right]^2\right\}^{1/2}}{A^*(x, y)}. \qquad (5)$$

Since

$$\frac{\partial I_1(x, y)}{\partial x} = 2A(x, y)\, y), \partial x), \qquad (6)$$

using the relation between $A(x, y)$ and $A^*(x, y)$, we finally obtain the expression:

$$\frac{\partial\varphi(x,\,y)}{\partial x} = \frac{\left\{4I_1(x,\,y)\,I_2(x,\,y) - c^2\left[\dfrac{\partial I_1(x,\,y)}{\partial x}\right]^2\right\}^{1/2}}{2c\,I_1(x,\,y)} \ . \qquad (7)$$

The quantities $I_2(x,\,y)$ and   differ in that the first quantity is the result of differentiation of an incident light beam, whereas the second quantity is the result of differentiation of an incoherent beam, i.e., of the incident beam that has been preliminary processed, e.g., transmitted through a light scattering transparency. The analogous expression for the y coordinate can be derived in a similar way.

A disadvantage of the above method is that further processing of the results is required to reconstruct the phase front, e.g., by the way suggested in Ref. 7. In this respect, it is analogous to the well–known Hartmann sensors. It is self–evident that the method entails additional computations.

This raises the question of a search for alternative procedures for processing of the measured intensity that, unlike the above method, would yield immediately the discrete values of field phase. A modified version of such a procedure for data processing, reported previously in Ref. 12, is described below.

Let us introduce designations for the Fourier transform of the complex amplitude $F(x,\,y)$:

$$G(u,\,v) = B(u,\,v)\,\exp\left(-\,i\,\xi(u,\,v)\right), \qquad (8)$$

where $B(u,\,v)$ and $\xi(u,\,v)$ are the amplitude and phase distribution measured, e.g., in the focal plane of a lens.

With the known functional relationship between $F(x,\,y)$ and $G(u,\,v)$, we can write

$$B(u,\,v) =$$

$$= \int_s\!\!\int A(x,\,y)\,\exp[-\,i\,\{\varphi(x,\,y)+(ux+vy)+\xi(u,\,v)\}]\,\mathrm{d}x\,\mathrm{d}y, (9)$$

where s is the area of the input aperture.

If an amplitude transparency having finite transmittance and dimensions $\Delta s = \Delta x\Delta y$ is placed in the plane of the input aperture of a lens at the point $(x_i,\,y_i)$, this results in a change of the given amplitude distribution of the Fourier transform. For a sufficiently low value of $(1-k)\Delta s$, where k is the transmittance of the transparency, we can write

$$\frac{[B(u,\,v) - B(u,\,v,\,x_i,\,\Delta x_i,\,y_i,\,\Delta y_i)]}{(1-k)\,A(x_i,\,y_i)\,\mathrm{D}s} \approx$$

$$\approx \cos[\varphi(x_i,\,y_i) + (u\,x_i + v\,y_i) + \xi(u,\,v)], \qquad (10)$$

where $B(u,\,v,\,x_i,\,\Delta x_i,\,y_i,\,\Delta y_i)$ is the amplitude distribution in the focal plane of the lens on condition that the transparency having finite transmittance and dimensions $\Delta x_i,\,\Delta y_i$ is placed in the aperture of the lens at the point $(x_i,\,y_i)$.

Formally speaking, the right–hand side of expression (10) can be obtained from Eq. (9) by differentiating its right–hand side with respect to the parameters s and $A(x_i,\,y_i)$. Let us multiply both sides of expression (10) by $\{B(u,\,v) + B(u,\,v,\,x_i,\,\Delta x_i,\,y_i,\,\Delta y_i)\}$ and introduce the following designations:

$$[B(u,\,v)]^2 = I(u,\,v)\ ,$$

$$[B(u,\,v,\,x_i,\,\Delta x_i,\,y_i,\,\Delta y_i)]^2 = I(u,\,v,\,x_i,\,\Delta x_i,\,y_i,\,\Delta y_i)\ ,$$

$$[A(x_i,\,y_i)]^2 = I(x_i,\,y_i)\ . \qquad (11)$$

Let us also consider that

$$B(u,\,v) + B(u,\,v,\,x_i,\,\Delta x_i,\,y_i,\,\Delta y_i) \approx 2B(u,\,v) \qquad (12)$$

as these amplitudes are close in values given that $(1-k)\Delta s$ is small. From the expression obtained as a result of the above manipulations, let us find $\varphi(x_i,\,y_i)$ and after its integrating over the u and v variables with consideration for the symmetry of a measuring system, we derive the final calculational relationship

$$\varphi(x_i,\,y_i) = \frac{1}{4u_1v_1} \times$$

$$\times \int_{-u_1}^{u_1}\!\int_{-v_1}^{v_1} \arccos\left\{\frac{I(u,\,v) - I(u,\,v,\,x_i,\,\Delta x_i,\,y_i,\,\Delta y_i)}{2\,(1-k)\,\Delta s[I(x_i,\,y_i)\,I(u,\,v)]^{1/2}}\right\}\mathrm{d}u\,\mathrm{d}v\ . \qquad (13)$$

The method described is advantageous. First, it eliminates the need for laborious procedure for reconstruction of the phase distribution, which can be obtained directly by performing measurements and calculations in accordance with Eq. (13). Secondly, this method is simple for practical implementation. The device intended for the implementation of the method comprises the following basic components: a lens, a recording device, and a dynamic transparency, e.g., a liquid crystal that is easy to make. The modification described herein differs from that reported earlier in that the transparency of finite transmittance is used in its design. In this case the condition that $(1-k)\Delta s$ should be small is much more easily satisfied than that for Δs. It is sufficient to choose a transparency having k value close to unity. A drawback of the method is that the sign of the phase is uncertain when passing through the center of the lens aperture in calculations. In practice, this uncertainty can easily be eliminated by performing surplus measurements.

4. CUMULANT METHODS FOR ASSESSING THE POTENTIAL CHARACTERISTICS OF AOS

AOS development brings up the question of their precision characteristics. This is due to the fact that AOS are fairly complex in structure. To analyze the precision characteristics, AOS can be tentatively divided into three subsystems:

– subsystem for recording of optical radiation with phase distortions;

– subsystem for phase–front reconstruction from measured and calculated components of the vector of control signals (in the case of multidither systems it is subsystem for shaping of test signals and vector of control actions);

– subsystem for correcting the phase distribution (as a rule, it is a flexible adaptive mirror).

The AOS subsystem for recording of optical radiation is generally a photodetector or a photodetector matrix. In the case of Poisson signal reception against the background of the Poisson noise, analysis of the potential characteristics of a photodetector is not unduly difficult. However, an

analysis of the Poisson noise statistics of quadrant photodetector, which is an integral part of the Hartmann sensor, is slightly more sophisticated problem. An original approach has been suggested by us for this particular case[13]; it is based on an analysis of the sum and difference of cumulants of the sought–for random Poisson process. Using the expressions obtained for distribution density, the structure for optimal estimation has been synthesized with proper allowance made for the sum–and–difference technique for the Poisson signal processing.

The accuracy characteristics of various algorithms for phase–front reconstruction have been analyzed in Refs. 6–10. As a result, the dependence of the following form has been found to exist:

$$\sigma^2 = G(N,\, \alpha)\, \sigma^2_{meas}\,, \qquad (14)$$

where σ^2 is the error variance of the phase front reconstruction; s^2_{meas} is the measurement variance; $G(N,\, \alpha)$ is a coefficient which depends, as a rule, on the number N of AOS control channels and on the other parameters of an α algorithm.

Analysis of AOS in terms of their precision characteristics for multidither probing reported in Refs. 14–17 is based on cumulant description of noise in AOS control channels. Briefly, the essential features of the method are as follows. The notion of a negative increment in the quality functional due to noise in AOS control channels ΔJ is introduced in the following form:

$$\Delta J = <J^0 - J>\,, \qquad (15)$$

where J^0 is the maximum value of the quality functional, J is the maximum value of the quality functional with noise observed in control channels. Angular brackets are used from here on to denote the mathematical expectation. Along with the mathematical expectation of ΔJ, its variance σ^2_Δ is also introduced. Obviously, the efficiency of various algorithms can be adequately assessed with the use of the above quantities. The method suggested allows us to find the values of ΔJ and σ^2_D when noise of different origin, e.g., Gaussian, Poisson, etc., is observed in control channels. All one has to do is to make a substitution of expressions for corresponding cumulants into the general expression, to transform this expression, and finally to undertake computer–aided analysis.

Analysis of the subsystem for phase–front correction, in addition to the problem of quality assessment of phase–front approximation by means of a specific adaptive mirror, poses the problem of optimizing the number of spatial modes of the mirror. The essence of the problem is as follows. The phase–front sensor measures local tilts of the phase front at N_1 points. The adaptive mirror has N_2 degrees of freedom, with $N_2 < N_1$. It is evident that as N_1 increases, σ^2 also would increase in accordance with expression (14), and an increase of N_2 would cause the error of phase–front approximation to reduce. Thus, we are dealing with classical problem of N_2 optimization for preassigned value of σ^2_{meas}. The problem of optimization has been solved for an adaptive mirror of arbitrary type.[18,19] A mathematical apparatus of normalized parabolic B–splines is used to describe the mirror surface. Its choice is stipulated by the fact that originally it was devised to describe membrane deformations. The descriptions of membrane deformations have been analyzed in terms of their accuracy. It has been found that in principle there is no point in increasing the power of spline in so far as this provides but an insignificant improvement in accuracy, while requires larger volume of calculations.

The method for selecting the number of spatial modes with allowance made for the noise of the Hartmann sensor[18,19] permits to restrict the number of degrees of freedom of arbitrary phase–front corrector based on specific conditions of AOS operation. Analysis has shown that in order to minimize the error variance resulting from system noise, in general it is necessary to increase the number of quadrant photodetectors of the Hartmann sensor.

With the spline–approximation method, it is possible, by using a numerical–analytical procedure, to find with a satisfactory accuracy the matrix components of a normal system of equations in the form of a linear combination of the normalized B–spline coefficients. In this case both the eigenvalues of response functions and their partial derivatives can be used as *a priori* information for constructing a spline to describe an adaptive mirror. It should be noted that the proposed method used for optimization of adaptive mirrors based on piezoelectric plates is also appropriate in the case of AOS having membrane–type mirrors that are controlled with actuators of different types.

5. NEW DESIGN FEATURES IN THE DEVELOPMENT OF ELEMENT BASE OF ADAPTIVE OPTICS

The development of a new element base plays a significant part in AOS creation. A segmented phase–front corrector is the simplest in design[4] (see Fig. 2). It incorporates 23 actuators 20×20 mm in size. The extreme angular actuators of 5×5 component aperture of the corrector are not included in order that aperture shape be near–circular. Three extra actuators are added that allow one to control the position of the aperture.

Use of circular piezoelectric plates turns out to hold more promise for the development of phase correctors. Figure 3 shows a flexible piezoelectric mirror,[20,21,22] which comprises a metal substrate clamped on a piezoelectric plate. The silver or aluminium electrodes are sprayed on the back side of the piezoelectric plate polished optically flat. The design developed is distinguished by the absence of an additional reflecting glass plate. This allowed us to obtain large deformations (to 50 μm) for an experimental model 50 mm in diameter,[20] with the frequency range extending up to 1 kHz. A series of flexible adaptive mirrors based on this design has been developed. Figure 4 shows a mirror having adjustable focal distance.[23] The piezoelectric actuator made up of a package of piezoelectric discs, with the thickness and diameter of the said discs being calculated using the procedure reported in Ref. 20. This design is advantageous in that the diameter of the working aperture of the mirror can exceed the maximum diameter of a commercially available piezoelectric plate by a factor of 1.5 to 2.
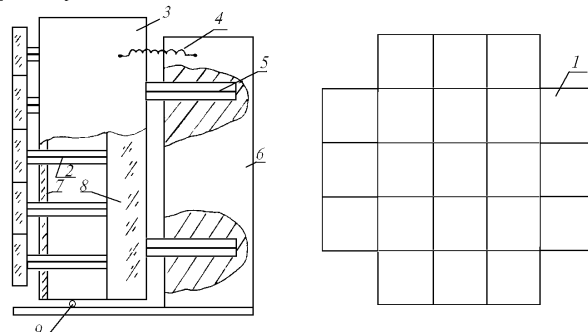

FIG. 2. *Segmented phase–front corrector: subapertures (1), piezoceramic actuators (2 and 5), housing (3), spring (4), base (6), system for applying controlling voltages at the actuators (7), intermediate base (8), and ball support (9).*
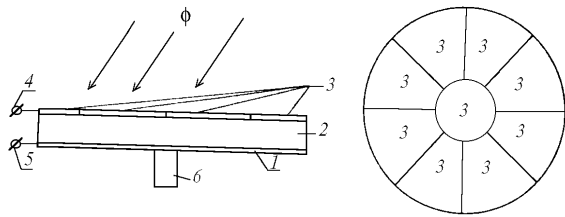
FIG. 3. Flexible piezoelectric mirror: metal substrate (1), piezoelectric plate (2), control electrodes (3), and terminals (4 and 5).
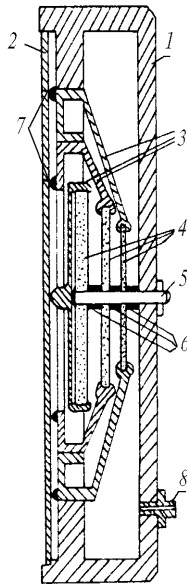

FIG. 4. Mirror with adjustable focal distance: housing (1), reflecting membrane (2), pushers (3), piezoelectric elements (4), axle (5), dielectric washers (6), conjugation components (7), and valve (8).

Figures 5a and b illustrate an adaptive mirror design available in two modifications,[5] i.e., a segmented corrector with shift and tilt control (a) and a mirror having continuous reflecting surface (b). This mirror can be directly controlled by signals from the Hartmann sensor. The device employs piezoelectric discs as active elements.[19]
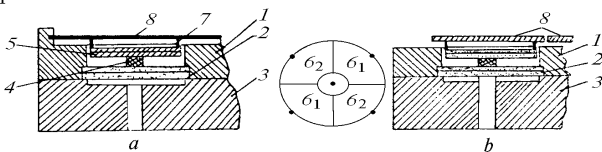

FIG. 5. Phase–front corrector with tilt and shift control and continuous reflecting coating (a) and segmented reflecting coating (b): 1) dielectric plate, 2) piezoelectric element for shift control, 3) housing, 4) support, 5) piezoelectric element for tilt control, 6) shape of control electrodes of the piezoelectric element 5, 7) rods, and 8) reflecting membrane.

Figure 6 depicts the design[24] of adaptive mirrors for large telescopes. This is distinguished by the use of hexagonal plates as active elements.[20] Piezoelectric plates are clamped on a massive base along generatrix. A constructional limitation on the size of the mirror (diameter of the aperture) is lifted owing to the use of several piezoelectric plates instead of one as an active element. In order to calculate the vector of control signals for such a mirror, it is expedient to use the mathematical apparatus of normalized B–splines.
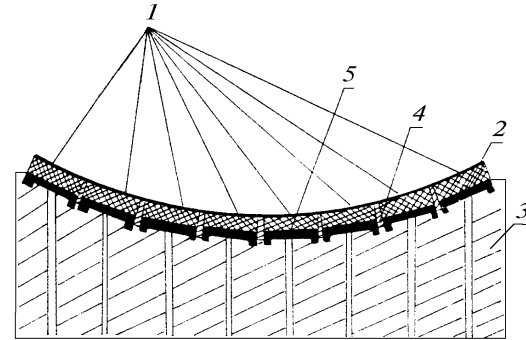

FIG. 6. Segmented parabolic mirror: reflecting coating (1), piezoelectric plates (2), base (3), dielectric inserts (4), and metal substrates (5).

Alongside with reflecting–type devices intended for correcting the phase distribution, various transmitting–type correctors are being developed, e.g., electrooptical $LiNbO_3$ crystals.[25] A phase corrector of this type is a collection of electrooptical crystals 30×20×2 in size. The said crystals have control electrodes sprayed on both sides, with the shape of the electrodes corresponding to the corrected mode (tilt, defocusing, etc.). An optical beam is squeezed with the aid of a cylindrical lens prior to correction. At the output of the crystal the beam reconstructs its original shape by means of a similar lens. The required number of crystals can be placed one after the other thereby providing a preset range and modes of phase correction.

The development of nearly all servomechanisms of AOS, i.e., piezoelectric elements, electrooptical crystals and Kerr cells, calls for the use of high voltages for their control (a few hundreds and thousands of volts at a frequency of up to 5 kHz). Thus, designers are faced with the problem of development of special–purpose amplifiers capable of carrying a capacitive load and providing high output voltages about a few thousands of volts.

We have developed an amplifier design,[26–29] the block diagram of which is shown in Fig. 7. Its operation has a distinctive feature, viz. as input voltage increases, the circuit "operational amplifier 1 – paraphase stage 2 – blocking oscillators 3" generates a pulse train to control chopper transistors of the output stage.
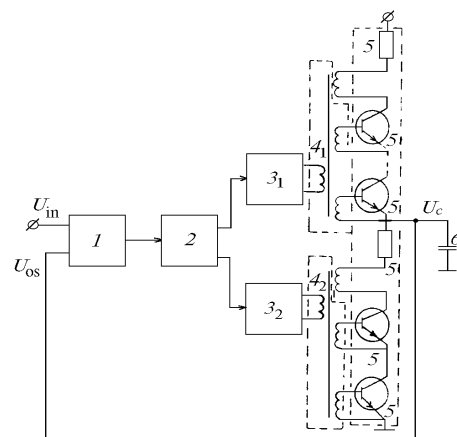

FIG. 7. Block diagram of a high–voltage amplifier: operational amplifier (1), paraphase stage (2), controlled oscillators (3), control windings of the output stage (4_1 and 4_2), transistors of the output stage (5), and capacitive load (6).

A salient feature of the amplifier circuit (Fig. 7) is variation of the repetition frequency of control pulses as a function of input signal shape (rate of its variation). In the special case in which this is insufficient for producing a respective control signal at the capacitive load, pulse duration also varies as a function of input signal shape. By combining the above design features, a high degree of linearity of the amplifier is attained. Owing to the use of the chopper output transistors, power dissipation is relatively small. The dimensions of the amplifier do not exceed 100×80×30 mm. In conclusion, it should be noted that the experimental studies reported in this review were performed using the above amplifiers.

6. DEVELOPMENT OF NEW AOS STRUCTURE BASED ON SYNTHESIZED ALGORITHMS

By and large, application of theoretical results to the development of new system structure is the ultimate goal of scientific work.

Block diagrams shown in Refs. 30 and 31 allow the practical implementation of the algorithm for piecewise–linear approximation of phase front of the form described in Ref. 6.

Figure 8 shows the block diagram of a phase–front sensor[32] in which the algorithm in the form of Eq. (1) is implemented.[1] The segmented phase–front corrector modulates each elementary section of the phase front with the frequency ω_i. The signal reflected from the corrector is recorded by the photodetector. A signal proportional to the intensity gradient at the point photodetector is separated using a system of bandpass filters. Weighting and forming of the vector of output signals are performed by means of units 8, 9, and 10, with the vector components being proportional to phase values at respective points of the aperture.
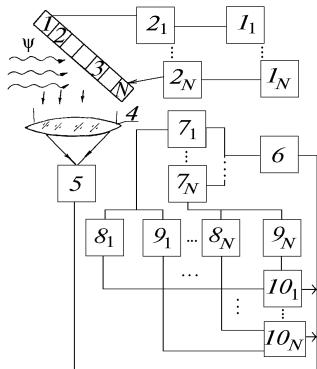

FIG. 8. Phase–front sensor: test–signal generators (1), amplifiers (2), segmented phase–front corrector (3), lens (4), point photodetector (5), preamplifier (6), bandpass filters (7), weighing elements (8 and 9), and adders (10).

The detector developed served as a basic unit around which a multidither system was built employing two adaptive mirrors: one with a wide frequency characteristic and a narrow dynamic range serves for modulating the optical radiation and for measuring the phase distribution on the aperture, and another with a narrower frequency characteristic and a wide dynamic range serves for actual correcting the phase–front distortions.

Figure 9 shows AOS structure with a flexible adaptive mirror.[33] The operation of this system is based on the algorithm described in Ref. 2. Actually, an additional number (m^2) of weighting elements 10 as well as corresponding links have been introduced into a multidither

system with multichannel phase modulation. Thus, a second–order gradient algorithm is implemented– in the given system, with the properties of a flexible adaptive mirror being taken into account.
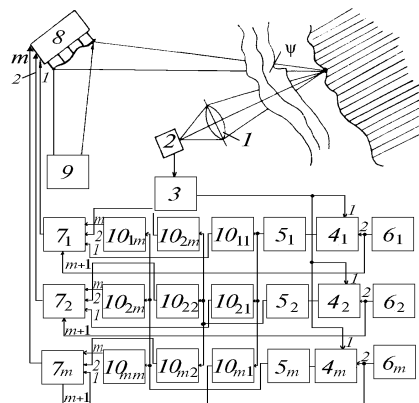

FIG. 9. Adaptive optical multidither system: lens (1), point photodetector (2), preamplifier (3), synchronous detectors (4), amplifiers (5), test–signal generators (6), adders (7), membrane–type adaptive mirror (8), laser (9), weighing elements (10), and turbulent atmosphere (ψ).

Figure 10 illustrates a phase–front sensor of interference type.[3,4] The operation of this device is as follows. An optical quantum generator and a beam stretcher form a reference beam that is phase–shifted with the aid of a phase transparency. The value of the phase shift depends on the channel number and is equal to $\Delta\varphi = i(\lambda)/m$, $i = \overline{1, m}$, where λ is the radiation wavelength of the optical quantum generator. The measurable phase front falls on optical splitters, whose splitting coefficients are equal to $k_i = 1/(m + 1 - i)$, $i = \overline{1, m}$. Obviously, for such splitting coefficients the intensity of the measurable beam would be evenly split among the m channels.
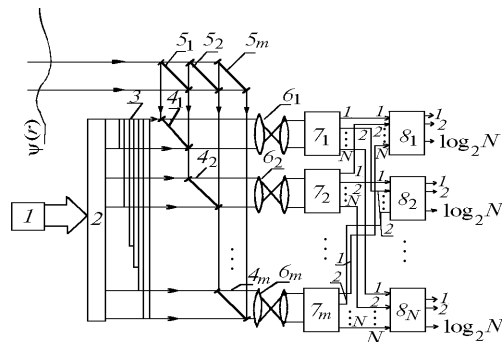

FIG. 10. Phase–front sensor of interference type: laser (1), collimator (2), collection of phase transparencies (3), semi–transparent mirrors (4 and 5), objectives (6), photodetector matrices (7), and scheme of phase value calculation (8).

After reflection from the semi–transparent mirrors and passage through the objectives, the measurable phase front interferes at the photodetector matrices with the reference front, which after passage through the phase transparency, the semi–transparent mirrors, and the objectives, is also incident on the photodetector matrices. The objectives serve for scaling of the measurable phase front and the

photodetector matrix. The comparison schemes convert the output signals to binary code corresponding to the phase shift on each matrix element of the photodetectors. Since the reference beam in all m channels of the device has different average phase, the interference patterns in the plane of photodetector matrix also would differ.

Let us consider the jth matrix element in all channels. Obviously, the maximum intensity would be observed in the channel in which the difference between the phase of the reference wave and that of the measurable phase front is the smallest. Thus, one of the jth signals would have a maximum value. In the jth comparison scheme, all m signals are compared and binary code that corresponds to the serial number of the channel with the maximum signal is formed at its output. Since the measurable phase value is unambiguously related to the serial number of channel, it can be defined as $\Delta\varphi = i\lambda/m = i\alpha$, $\alpha = \lambda/m$. In many instances this scaling is unnecessary, for the digital signal, corresponding to the phase of the jth matrix element, can be directly used to control AOS.

7. CONCLUSION

Because of limitations on the length of the paper, we cannot cover in detail the results obtained. Therefore, we have focused our attention on unpublished data. However, we would like to believe that the results might be of interest for workers engaged in theoretical and experimental investigations in the field of adaptive optics.

It should be noted that, on the whole, investigations have led to the development of devices and systems capable of fulfilling their functions as such and, above all, have broadened the scope of this field of knowledge. Both the theory and devices developed, in particular, systems intended for measurement and reconstruction of the phase front, can be used to advantage in fundamental investigations of the atmosphere, e.g., for studying vortex formation, since vortices by their nature are analogous to phase objects and cannot be visualized under natural conditions.

REFERENCES

1. D.A. Bezuglov, Kvant. Elektron. **16**, No. 8, 1612–1616 (1989).
2. D.A. Bezuglov, Kvant. Elektron. **17**, No. 3, 370–373 (1990).
3. T. O'Meara, in: *Adaptive Optics*, ed. E.A. Vitrichenko (Mir, Moscow, 1980).
4. D.A. Bezuglov, E.N. Mishchenko, and V.L. Tyurikov, Atm. Opt. **3**, No. 2, 184–186 (1990).
5. D.A. Bezuglov and E.N. Mishchenko, "Mirror wave–front corrector," Inventor's Certificate No. 1781662, Bull. No. 46, 1992.
6. D.A. Bezuglov, E.N. Mishchenko, and O.V. Serpeninov, Atm. Opt. **4**, No. 2, 137–140 (1991).
7. D.A. Bezuglov, Avtometriya, No. 2, 21–25 (1990).
8. D.A. Bezuglov and E.N. Mishchenko, in: Abstracts of Reports at the International Conference on Coherent and Nonlinear Optics "KiNO – 91" (GOI, Leningrad, 1991), pp. 90–91.
9. D.A. Bezuglov and E.N. Mishchenko, Izv. RAN, ser. Fiz. **56**, No. 12, 156–160 (1992).

10. D.A. Bezuglov and A.A. Vernigora, Atm. Opt. **3**, No. 3, 251–251 (1990).
11. S.E. Mishchenko, B.G. Saprunov, and Yu.P. Rondin, *"A technique for analyzing wave fronts of light fields,"* Positive Decision on Inventor's Application No. 4941728, Priority of June 3, 1991.
12. D.A. Bezuglov, E.N. Mishchenko, and S.E. Mishchenko, Atmos. Oceanic Opt. **5**, No. 12, 841–842 (1992).
13. D.A. Bezuglov and E.N. Mishchenko, Atmos. Oceanic Opt. (in print).
14. D.A. Bezuglov, Izv. RAN, ser. Fiz. **56**, No. 9, 225–229 (1992).
15. D.A. Bezuglov, Atm. Opt. **2**, No. 8, 683–686 (1989).
16. D.A. Bezuglov, Proc. SPIE (1992).
17. D.A. Bezuglov, in: *Abstracts of Reports at the International Conference on Coherent and Nonlinear Optics "KiNO – 91"* (GOI, Leningrad, 1991), pp. 90–91.
18. D.A. Bezuglov, in: *Abstracts of Reports at the XIth All–Union Symposium on Propagation of Laser Radiation in the Atmosphere and Aqueous Media* (Tomsk Affiliate of the Siberian Branch of the Academy of Sciences of the USSR, Tomsk, 1991), p. 218.
19. D.A. Bezuglov, Atm. Opt. **4**, No. 12, 900–904 (1991).
20. D.A. Bezuglov, Z.P. Mastorpas, and E.N. Mishchenko, *"Mirror wave–front corrector,"* Inventor's Certificate No. 1695252, Bull. No. 44, 1991.
21. D.A. Bezuglov, Z.P. Mastorpas, E.N. Mishchenko, et al., Atm. Opt. **2**, No. 12, 1119–1123 (1989).
22. D.A. Bezuglov and E.N. Mishchenko, Atm. Opt. **3**, No. 12, 1198–1199 (1990).
23. D.A. Bezuglov and E.N. Mishchenko, *"Mirror with adjustable focal distance,"* Positive Decision on Inventor's Application No. 5047407, Priority of June 15, 1992.
24. D.A. Bezuglov, E.N. Mishchenko, and I.A. Sysoev, "Mirror wave–front corrector," Positive Decision on Inventor's Application No. 50512083, Priority of July 6, 1992.
25. D.A. Bezuglov, Z.P. Mastorpas, E.N. Mishchenko, et al., Atm. Opt. **3**, No. 7, 664–668 (1990).
26. D.A. Bezuglov, S.A. Eresko, and E.N. Mishchenko, Prib. Tekh. Eksp., No. 4, 125–126 (1990).
27. D.A. Bezuglov and E.N. Mishchenko, Prib. Tekh. Eksp., No. 1, 145–148 (1993).
28. D.A. Bezuglov and E.N. Mishchenko, in: Abstracts of Reports at the XIth All–Union Symposium on Propagation of Laser Radiation in the Atmosphere and Aqueous Media (Tomsk Affiliate of the Siberian Branch of the Academy of Sciences of the USSR, Tomsk, 1991), p. 218.
29. D.A. Bezuglov, E.N. Mishchenko, and S.E. Mishchenko, "High–voltage dc amplifier," Inventor's Certificate No. 1802396, Bull. No. 10, 1993.
30. D.A. Bezuglov, E.N. Mishchenko, M.I. Krymskii, et al.,*"Wave–front sensor,"* Inventor's Certificate No. 1720051, Bull. No. 10, 1992.
31. D.A. Bezuglov, E.N. Mishchenko, and V.L. Tyurikov, *"Wave–front sensor,"* Inventor's Certificate No. 1647496, Bull. No. 17, 1991.
32. D.A. Bezuglov, *"Wave–front sensor,"* Inventor's Certificate No. 1559925.
33. D.A. Bezuglov, E.N. Mishchenko, and V.L. Tyurikov, *"Adaptive optical system,"* Inventor's Certificate No. 161629.
34. D.A. Bezuglov, E.N. Mishchenko, and V.L. Tyurikov, *"Wave–front sensor,"* Inventor's Certificate No. 1664044.